CALPHAD: Computer Coupling of Phase Diagrams and Thermochemistry 56 (2017) 102–107

Contents lists available at ScienceDirect

CALPHAD: Computer Coupling of Phase Diagrams and Thermochemistry

journal homepage: www.elsevier.com/locate/calphad

Thermodynamic modelling of Ti-Zr-N system

Soumya Sridar*, Ravi Kumar, K.C. Hari Kumar

Department of Metallurgical and Materials Engineering, Indian Institute of Technology Madras, Chennai 600036, India

ARTICLE INFO

Keywords:
Calphad
ab initio
Zr-N
Ti-Zr
Ti-Zr-N

ABSTRACT

Thermodynamic modelling of Ti-Zr-N system is performed using Calphad method coupled with *ab initio* calculations. The energies of formation of stable and metastable end-members of sublattice formulations of solid phases in Zr-N system and enthalpy of mixing of the mixed nitride (Ti, Zr)N (δ) are calculated using *ab initio* method. Phonon calculations are used to compute the Gibbs energies of stoichiometric ZrN and the mixed nitride δ. With the aid of experimental thermochemical and constitutional data from the literature along with the results of *ab initio* calculations, thermodynamic optimization is carried out to obtain the Gibbs energy model parameters.

1. Introduction

Transition metal nitride coatings are of great interest in applications like cutting and forming tools due to their high hardness and wear resistance. Titanium nitride (TiN) coatings are currently used in these applications and studies on improving these coatings is predominantly focused on TiN-based alloy coatings and multi layers [1]. (Ti,Zr)N is one such system that is of interest due to its elevated temperature mechanical and tribological properties [2]. It has been observed that (Ti,Zr)N coated cemented carbide tips showed improved cutting performance, which is attributed to the alloying effect of Zr with Ti in fcc-TiN unit cell [3]. It has also been observed that if high temperatures are achieved at chip-tool contact zone, owing to the high cutting speed, spinodal decomposition can occur at the contact zone, which leads to further increase in hardness and wear resistance [4]. Hence, the knowledge of phase equilibria will be helpful in understanding the phase evolution and fine-tuning the chemistry of these coatings in order to enhance its properties.

2. Binary systems

2.1. Ti-N system

There are five equilibrium phases present in this system: liquid, (βTi), (αTi), TiN and Ti_2N. In the present work the Gibbs energy description by [5] is used. The corresponding calculated phase diagram is shown in Fig. 1.

2.2. Ti-Zr system

The phase diagram of this system is relatively simple with three phases namely liquid, (βTi, βZr) and (αTi, αZr). Gibbs energy description by [6] is revised here mainly to have better agreement with the enthalpy of mixing of liquid phase measured subsequently by [7].

2.3. Zr-N system

The Zr-N phase diagram, which was modelled initially by [8,9] and subsequently improved by [10]. It is re-assessed here mainly because some critical experimental data available in the literature was not used for optimization by [10]. The crystallographic data for the equilibrium phases in this system are summarized in Table 1. The sources of constitutional data for this system are given in Table 2. Table 3 lists the details of the co-ordinates of invariant equilibria reported in the literature. The sources of experimental thermochemical data for different phases are listed in Table 4. The melting temperature of ZrN was reported as ≈3273 K at 1 atm by [11] and was measured to be around 3670 K at pressure slightly greater than 60 atm by [12].

3. Ternary system

Only limited experimental information is available for Ti-Zr-N system. According to [27] mono nitrides of titanium and zirconium are completely miscible at 2000 K. Later studies by [28] indicated that the ternary mixed nitride δ is immiscible at least till 2000 K. There is no experimental data on the coordinates of critical point of the miscibility gap. However, there are several *ab initio* calculations related

* Corresponding author.
E-mail address: soumya_sridar@yahoo.co.in (S. Sridar).

http://dx.doi.org/10.1016/j.calphad.2016.12.003
Received 30 September 2016; Received in revised form 23 November 2016; Accepted 14 December 2016

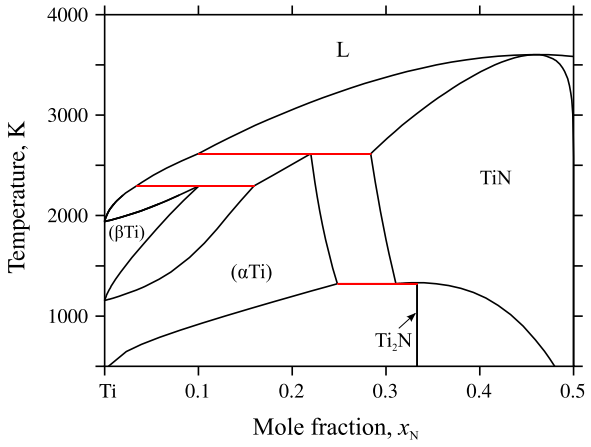

Fig. 1. Calculated Ti-N phase diagram [5].

Table 1
Zr-N: details of solid phases [13].

Phase	Composition (at% N)	Pearson symbol	Space group
(βZr)	0–5	cI2	$Im\bar{3}m$
(αZr)	0–24.7	hP2	$P6_3/mmc$
ZrN	40–50	cF8	$Fm\bar{3}m$

Table 2
Zr-N: summary of constitutional data.

Phase boundary measured	Method	Reference
L/L+(βZr)	Incipient melting	[14]§
L/L+(αZr)	Incipient melting	[14]§
L/L+ZrN	Incipient melting	[14]§
(βZr)/(βZr)+(αZr)	Metallography	[14]
(βZr)+(αZr)/(αZr)	Metallography	[14]
(αZr)/(αZr)+ZrN	Metallography	[14]
Zr-rich boundary of ZrN	Metallography, XRD	[14]§
	Metallography, XRD	[15]§
	Vapour pressure, XRD	[16]
	Vapour pressure	[17]§
	XRD, hardness, electrical resistivity	[18]

§ Data not taken into account by [10].

Table 3
Zr-N: co-ordinates of invariant equilibria [14].

Equilibrium	Composition (at% N)	Temperature (K)
L + (αZr) ⇋(βZr)	4.4 ± 0.7, 16.8 ± 0.7, 5 ± 1.1	2153 ± 10
L + ZrN ⇋(αZr)	13.8 ± 0.7, 40 [18], 24.7 ± 1.7	2261 ± 15

to this in the literature. These are summarized in Table 5. Partial ($Ti_{0.5}Zr_{0.5}$)-N isopleth was determined experimentally by [29]. Since, the duration of isothermal nitridation is not mentioned, it is not clear whether the equilibrium is achieved in those studies. Hence, their data is not considered in this work.

4. Thermodynamic models

Gibbs energy functions for the elements are from the SGTE compilation [33]. The sublattice formulation used for modelling Gibbs energies of various phases in Zr-N, Ti-Zr and Ti-Zr-N system are summarized in Table 6.

The liquid phase is modelled using a single lattice random substitutional solution and the terminal solid solution phases are

Table 4
Zr-N: summary of experimental thermochemical data.

Phase	Quantity	Composition (at% N)	Reference
ZrN	$\Delta_f H_{298}^\circ$	50	[18]
			[19]
			[20]§
			[21]§
			[22]§
			[23]§
		43.5– 47.1	[19]§
		40.8– 42.5	[18]§
ZrN	$C_{p,298}^\circ$	50	[24]
ZrN	S_{298}°	50	[25]
ZrN	$H_T^\circ - H_{298}^\circ$	50 (371–1672 K)	[26]§
ZrN		41.9–49 (1204 – 2387 K)	[24]§
ZrN	p_{N_2}	45–49.5	[12]§
(αZr)	$\Delta_f H_{298}^\circ$	9.9–14.5	[19]§

§ Data not taken into account by [10].

Table 5
Ab initio predictions of critical point of the miscibility gap in the δ phase of TiN-ZrN system.

Critical point		Reference
T (K)	(x_{ZrN})	
5000	0.36	[30]
2670	0.35	[31]
1880*	0.35	[31]
1920	–	[32]

* With vibration contribution.

Table 6
Sublattice formulations used for various phases in this work.

Phase	Sublattice formulation
Zr-N	
Liquid	$(N, Zr)_1$
(αZr)	$(Zr)_1 (N, Va)_{0.5}$
(βZr)	$(Zr)_1 (N, Va)_3$
ZrN	$(Zr)_1 (N, Va)_1$
Ti-Zr	
Liquid	$(Ti, Zr)_1$
(αTi, αZr)	$(Ti, Zr)_1 (Va)_{0.5}$
(βTi, βZr)	$(Ti, Zr)_1 (Va)_3$
Ti-Zr-N	
Liquid	$(N, Ti, Zr)_1$
(αTi, αZr)	$(Ti, Zr)_1 (N, Va)_{0.5}$
(βTi, βZr)	$(Ti, Zr)_1 (N, Va)_3$
δ	$(Ti, Zr)_1 (N, Va)_1$

modelled with two sublattices, one occupied by Ti and Zr and the other by N and vacancy (Va). The excess Gibbs energy for these phases are expressed using Redlich-Kister-Muggianu scheme [34,35].

5. *Ab initio* calculations

The experimental thermochemical data available for Zr-N and Ti-Zr-N systems are rather limited. Hence, we performed *ab initio* calculations to the obtain thermochemical properties in these systems. All calculations at 0 K were carried out using Vienna Ab initio Simulation Package (VASP) [36,37] supplied with MedeA [38] user interface. The VASP input parameters used in this study for relaxing the structures are listed in Table 7. The enthalpy of formation of a

Table 7
VASP input parameters.

Potential	PAW [40,41]
Exchange-correlation functional	GGA-PBE [42]
Energy cut-off	600 eV
k-point spacing	≤0.2 Å^{-1}
k-point sampling scheme	Monkhorst-Pack [43]
Geometric convergence	0.002 eV/Å
SCF convergence	10^{-7} eV
Integration scheme	Tetrahedron with Blöchl correction [44]

Table 8
Enthalpy of formation of end-members in Zr-N system.

End-member	$\Delta_f H^\circ_{298}$ (J/mol)
ZrN	−341,593
$ZrN_{0.5}$	−148,695
ZrN_3	+280,996

phase is approximated from the total energy at 0 K (E_0) using the following equation.

$$\Delta_f H^\circ_{298}(\text{phase}) \approx E_0(\text{phase}) - \sum_{i=\text{elements}} \nu_i E_0(i) \quad (1)$$

where ν_i are the stoichiometric coefficients of the constituent elements in the phase of a chosen stoichiometry. The enthalpy of formation of various end-members in the sublattice formulation of phases in Zr-N system, calculated using Eq. (1), are given in Table 8. The enthalpies were calculated with respect to hcp-Zr and N_2(g). The total energy calculations for N_2(g) were done according to the procedure given in [39]. Hcp-Zr with half the octahedral voids filled with nitrogen and bcc-Zr with all the octahedral voids filled with nitrogen was considered for total energy calculations of $ZrN_{0.5}$ and ZrN_3 end-members, respectively.

In order to compute the enthalpy of mixing of TiN and ZrN, special quasirandom structures (SQS) [45] was used to model the random distribution of metal atoms in the nitride solid solution. 16-atom SQS structures were generated using *mcsqs* code [46] of Alloy Theoretic Automated Toolkit (ATAT) [47]. The crystal structure of the mixed nitrides obtained were triclinic and the correlation functions for different configurations mimic the correlation function of the random alloy for first few nearest neighbours. The structures were fully relaxed and the enthalpy of mixing is calculated using the following equation.

$$\Delta_{\text{mix}} H^\circ_{298}(\delta) \approx E_0(\text{Ti}_x\text{Zr}_{1-x}\text{N}) - xE_0(\alpha\text{Ti}) - (1-x)E_0(\alpha\text{Zr}) - 0.5E_0(\text{N}_2(\text{g})) \quad (2)$$

The calculated enthalpy of mixing (Fig. 2) using Eq. (2) indicates demixing of the binary nitrides.

The finite temperature thermodynamic properties were estimated using harmonic approximation as implemented in the PHONON code [48] supplied with MedeA. A 2 × 2 × 2 supercell and 2 × 2 × 1 supercell with 64 atoms were employed for stoichiometric ZrN and SQS structures of mixed nitrides, respectively. The Hellmann-Feynman forces were calculated by displacing the atoms from its equilibrium position with an amplitude of ± 0.02 Å. In the present work, harmonic approximation is used rather than quasiharmonic approximation, which is considered to be more accurate, since it will be computationally more intensive to implement the latter for SQS structures. Also, the Gibbs energy obtained using harmonic approximation (PHONON [48]) was found to be 0.2 and 4 kJ/mol of atoms higher at 300 and 3000 K, respectively, in comparison with Gibbs energy estimated using quasi-harmonic approximation (Phonopy [49]) for stoichiometric ZrN. Hence, harmonic approximation was found to be sufficiently accurate for the present purpose.

The Helmholtz energy (A°_T) obtained as a function of temperature from these calculations were transformed to Gibbs energy with respect to the so-called Standard Element Reference (SER) using the following equation [50].

$$G^\circ_T(\text{phase}) - \sum_{i=\text{elements}} \nu_i H^\circ_{298}(i) = E_0(\text{phase}) + \text{ZPE}(\text{phase}) + A^\circ_T(\text{phase}) - \sum_{i=\text{elements}} \nu_i [E_0(i) + \text{ZPE}(i) + (H^\circ_{298} - H^\circ_0)(i) + (pV(i))] \quad (3)$$

where ZPE is the zero point energy. The values for $(H^\circ_{298} - H^\circ_0)$ are taken from the SGTE compilation [33] and the ZPE are obtained from the phonon calculations. For nitrogen molecule, the zero point energy is obtained using the experimental vibrational frequency at 0 K [51]. The pV term is evaluated only for nitrogen, which is treated as an ideal gas. Hence, its value is calculated using the ideal gas equation. The Gibbs energy calculated using Eq. (3) for stoichiometric ZrN and δ ($Zr_{0.25}Ti_{0.75}N$) is shown in Fig. 3. The phonon calculations for other SQS structures of δ failed due to the occurrence of negative phonon frequencies.

6. Optimization

The Gibbs energy model parameters for Ti-Zr, Zr-N and Ti-Zr-N systems are optimized using PARROT module [52] of the Thermo-Calc software [53].

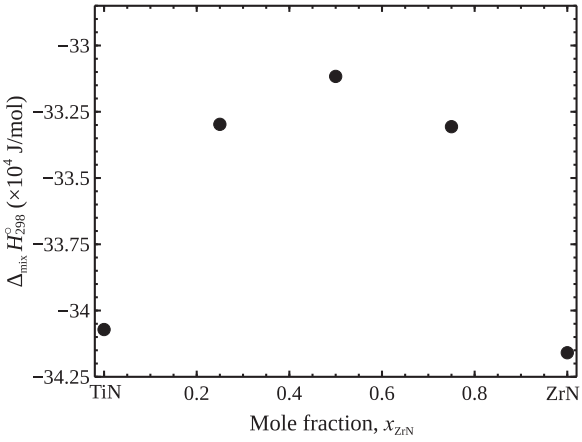

Fig. 2. Enthalpy of mixing of (Ti, Zr)N phase (δ) calculated using SQS.

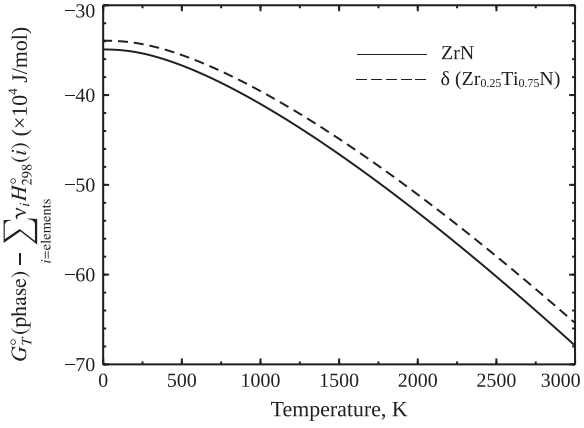

Fig. 3. Gibbs energy obtained from phonon calculations.

6.1. Zr-N

The experimental thermochemical and phase diagram data from literature along with the results from *ab initio* calculations obtained from this work were used as input in the optimization of Zr-N system. Since ZrN had relatively large amount of thermochemical data, the parameters for this phase was first optimized. Subsequently, the enthalpy parameters for (αZr) and (βZr) phases were optimized with the metastable end-member formation energies obtained from *ab initio* calculations. Using the constitutional data, the alternate mode of PARROT was used for generating the start values for the parameters of liquid phase and the remaining parameters of (αZr), (βZr) and ZrN phases and were further optimized using the full mode. Finally, by including all the model parameters and data, optimization was carried out and the parameters were rounded off according to the standard deviation criterion suggested by [54].

6.2. Ti-Zr

Ti-Zr system was optimized using experimental thermochemical and constitutional data. Liquid phase was chosen to be optimized first due to the availability of thermochemical data. Subsequently, the parameters of (αTi, αZr) and (βTi, βZr) phases were optimized with the help of alternate mode followed by full mode.

6.3. Ti-Zr-N

The thermodynamic descriptions of Zr-N and Ti-Zr obtained in the present work and Gibbs energy description of Ti-N from [5] were combined according to the Muggianu scheme to form an initial description for the ternary. The enthalpy of mixing of the binary nitrides and Gibbs energy of the ternary nitride (δ) obtained from *ab initio* calculations were used to optimize the ternary parameters for δ. All the optimized parameters obtained in this work are listed in Table 9.

Table 9
Gibbs energy parameters (in SI units) obtained in the present work.

Zr-N
Liquid: $(N, Zr)_1$
${}^0L^{Liquid}_{N,Zr}$=−427557
${}^1L^{Liquid}_{N,Zr}$=−153838
HCP_A3: $(Zr)_1$ $(N, Va)_{0.5}$
${}^0G^{HCP\_A3}_{Zr:N}$=GHSERZR + 0.5GHSERNN − 150903 + 43.853 T
${}^0L^{HCP\_A3}_{Zr:N,Va}$=−139011 + 45.439 T
${}^1L^{HCP\_A3}_{Zr:N,Va}$=−41938
BCC_A2: $(Zr)_1$ $(N, Va)_3$
${}^0G^{BCC\_A2}_{Zr:N}$=FT + 2GHSERNN + 632009 + 320.432 T
${}^0L^{BCC\_A2}_{Zr:N,Va}$=−1508137
FCC_A1: $(Zr)_1$ $(N, Va)_1$
${}^0G^{FCC\_A1}_{Zr:N}$=FT
${}^0L^{FCC\_A1}_{Zr:N,Va}$=+19575
FT = −367080.182 + 278.330233 T − 46.4312194 $T\ln(T)$ − .00352792791 T^2
+1.33236681E − 09 T^3 + 358416.094 T^{-1}(298.15 < T < 2000)
−309671.768 − 11.4672139 T − 9.01132806 $T\ln(T)$ − .0142983599 T^2
+5.79050986E − 07 T^3 − 16048445 T^{-1}(2000 < T < 2600)
−357218.131 + 237.61238 T − 41.3250297 $T\ln(T)$ − .00469480362 T^2
+5.0809381E − 08 T^3 − 3201806 T^{-1}(2000 < T < 3225)
−302090.81 + 345.052575 T − 58.5870002 $T\ln(T)$(3225 < T < 5000)
Ti-Zr
Liquid: $(Ti, Zr)_1$
${}^0L^{Liquid}_{Ti,Zr}$=−20278 + 8.427 T
HCP_A3: $(Ti, Zr)_1$ $(Va)_{0.5}$
${}^0L^{HCP\_A3}_{Ti,Zr:Va}$=+5707 − 2.403 T
BCC_A2: $(Ti, Zr)_1$ $(Va)_3$
${}^0L^{BCC\_A2}_{Ti,Zr:Va}$=−4100 + 3.470 T
Ti-Zr-N
FCC_A1: $(Ti, Zr)_1$ $(N, Va)_1$
${}^0L^{FCC\_A1}_{Ti,Zr:N}$=+26027
${}^1L^{FCC\_A1}_{Ti,Zr:N}$=+8468

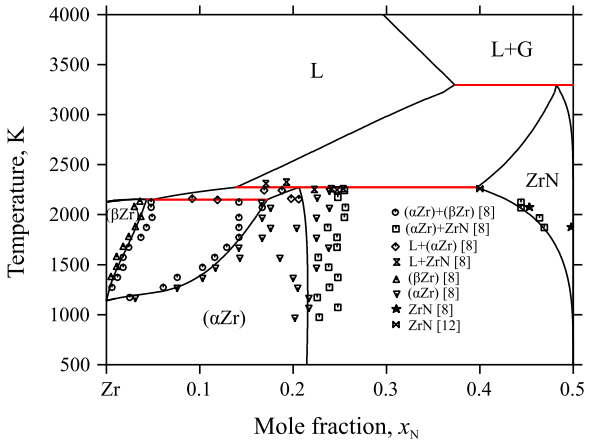

Fig. 4. Comparison of calculated Zr-N phase diagram with experimental data.

7. Results

The calculated phase diagram of Zr-N system using the parameters listed in Table 9 and its comparison with experimental data is shown in Fig. 4. It can be observed that there is reasonably good agreement between the experimental constitutional data and the calculated phase boundaries. According to [14], the invariant reaction (L+(αZr)⇋(βZr)) occurring at 2153 K is peritectic. From Table 3, it can be observed that the composition of liquid and (βZr) phases are very close for this invariant reaction. Considering the reported error, the reaction can be either eutectic or peritectic. Using these values as input in the optimization, the nature invariant reaction changed from peritectic to eutectic (L⇋(αZr)+(βZr)) in the present work. We found that forcing the reaction to be peritectic makes it very difficult to fit. In Hf-N system, a similar eutectic reaction occurs at 2463 K [55]. Since, Hafnium and Zirconium are elements which are similar in their chemical nature, it can be expected that the nature of invariant reaction in Zr-N system can also be eutectic, with the available experimental data. The comparison of experimental, *ab initio* and optimized values of enthalpy of formation of the stable end-member ZrN is given in Table 10. It can be observed that the optimized value falls within the range of measured experimental enthalpies and is in reasonably good agreement with the *ab initio* value. The calculated Gibbs energy of stoichiometric ZrN fits reasonably well with the values obtained from *ab initio* calculations at low temperature and fits accurately at high temperature as shown in Fig. 5.

The comparison of calculated phase diagram with experimental data [56–62] for Ti-Zr system is shown in Fig. 6. The calculated

Table 10
Comparison between experimental, theoretical and optimized values of enthalpies of formation of ZrN.

Method	$\Delta_f H^\circ_{298}$ (J/mol)
Calphad	−350,444
Ab initio	−341,593
Experimental	−336,519 [20]
	−339,532 [18]
	−343,800 [22]
	−364,700 [23]
	−365,263 [21]
	−369,030 [19]

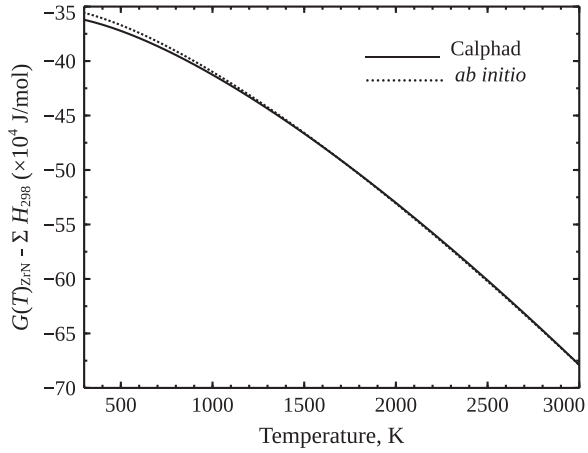

Fig. 5. Comparison of calculated and *ab initio* estimated Gibbs energy of ZrN.

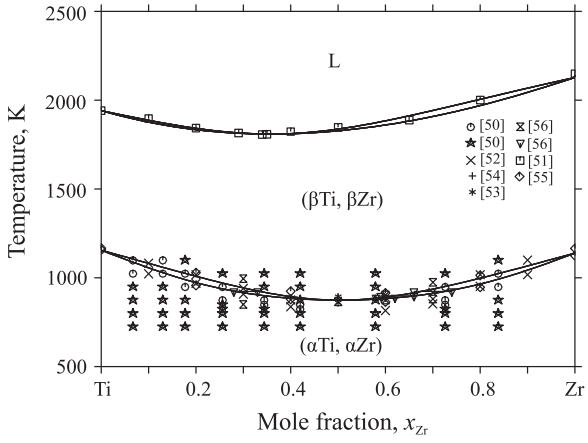

Fig. 6. Comparison of calculated Ti-Zr phase diagram with experimental data.

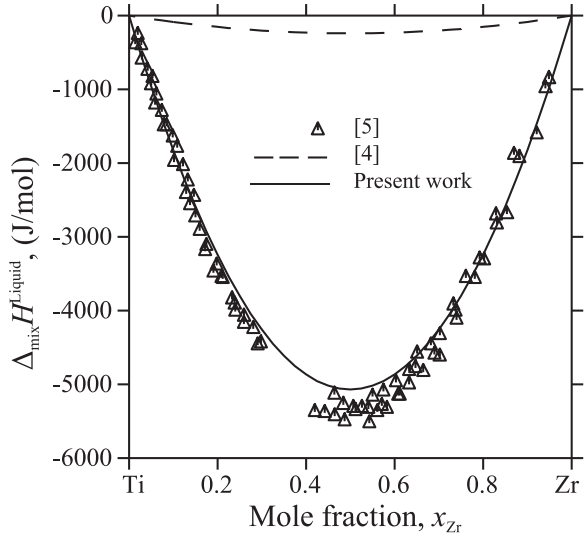

Fig. 7. Calculated and experimental values of enthalpy of mixing of liquid in Ti-Zr system.

enthalpy of mixing of liquid from the present work agrees well with the experimental data in comparison with the previous assessment as shown in Fig. 7.

The calculated TiN-ZrN section using the model parameters obtained in this work is shown in Fig. 8. The critical temperature and composition of miscibility gap was found to be 1844 K and 0.34 (x_{ZrN}), respectively. With reference to Table 5, the obtained values are

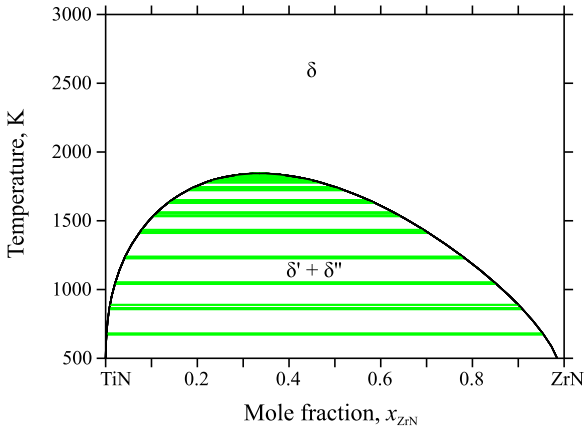

Fig. 8. Calculated TiN-ZrN section.

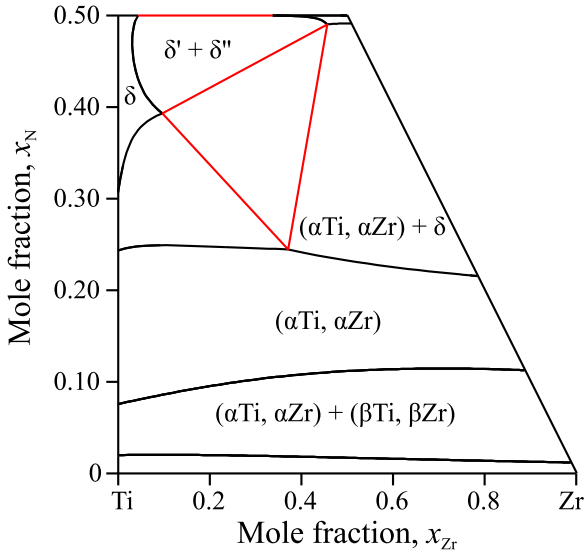

Fig. 9. Calculated partial isothermal section at 1473 K.

in reasonable agreement with the predictions of [31] since SQS method was used in that work as well. The critical temperature was overestimated by [30] under the assumption of ideal solution behaviour and underestimated by [32] using supercell method. This could be due to the method used for modelling the random metal atom sites in the mixed nitride. The partial isothermal section at 1473 K shown in Fig. 9 indicates the presence of δ-phase miscibility gap at that temperature.

8. Conclusions

Zr-N system is re-assessed with experimental information from literature augmented with thermodynamic properties obtained from *ab initio* calculations. Ti-Zr system was re-assessed by including recent thermochemical information that was not available at the time of previous assessment. The calculated phase diagrams are in good agreement with the experimental data. Gibbs energy parameters for Ti-Zr-N system are optimized using thermochemical data obtained from *ab initio* calculations. The calculated critical temperature and composition for miscibility gap matches well with the *ab initio* predictions reported in the literature. However, existence of the δ phase miscibility gap needs to be corroborated by experiments.

Acknowledgements

Financial support received from the Indo-French Centre for the Promotion of Advanced Research (IFCPAR/CEFIPRA) (Project No.

5108-1) is gratefully acknowledged.

Appendix A. Supplementary data

Supplementary data associated with this article can be found in the online version at http://dx.doi.org/10.1016/j.calphad.2016.12.003.

References

[1] I. Grimberg, V. Zhitomirsky, R. Boxman, S. Goldsmith, B. Weiss, Multicomponent Ti–Zr–N and Ti–Nb–N coatings deposited by vacuum arc, Surf. Coat. Technol. 108 (1998) 154–159.

[2] D.-Y. Wang, C.-L. Chang, C.-H. Hsu, H.-N. Lin, Synthesis of (Ti, Zr) N hard coatings by unbalanced magnetron sputtering, Surf. Coat. Technol. 130 (2000) 64–68.

[3] O. Knotek, M. Böhmer, T. Leyendecker, F. Jungblut, The structure and composition of Ti-Zr-N, Ti-Al-Zr-N and Ti-Al-V-N coatings, Mater. Sci. Eng., A 105 (1988) 481–488.

[4] O. Knotek, A. Barimani, On spinodal decomposition in magnetron-sputtered (Ti, Zr) nitride and carbide thin films, Thin Solid Films 174 (1989) 51–56.

[5] S. Jonsson, Assessment of the Ti-N system, Z. Metallkd. 87 (1996) 691–702.

[6] K.C. Hari Kumar, P. Wollants, L. Delaey, Thermodynamic assessment of the Ti-Zr system and calculation of the Nb-Ti-Zr phase diagram, J. Alloys Compd. 206 (1994) 121–127.

[7] U. Thiedemann, M. Roesner-Kuhn, K. Drewes, G. Kuppermann, M.G. Frohberg, Mixing enthalpy measurements of liquid Ti-Zr, Fe-Ti-Zr and Fe-Ni-Zr alloys, Steel Res. 70 (1999) 3–8.

[8] L. Gribaudo, D. Arias, J. Abriata, The N-Zr (nitrogen-zirconium) system, J. Phase Equilib. 15 (1994) 441–449.

[9] W.-E. Wang, D.R. Olander, Computational thermodynamics of the Zr-N system, J. Alloys Compd. 224 (1) (1995) 153–158.

[10] X. Ma, C. Li, K. Bai, P. Wu, W. Zhang, Thermodynamic assessment of the Zr-N system, J. Alloys Compd. 373 (2004) 194–201.

[11] O. Kubaschewski-von Goldbeck, Zirconium: Physico chemical properties of its compounds and alloys, Atomic Energy Review, Special issue No. 6, International Atomic Energy Agency, Vienna, 1976.

[12] M. Erop'yan, R. Avarbe, High-temperature region of stable existence of zirconium mononitride, Inorg. Mater. (USSR)(Engl. Transl.) 10 (1975) 1850–1852.

[13] P. Villars, K. Cenzual, Pearson's Crystal Data-Crystal Structure Database for Inorganic Compounds (on DVD), ASM International, Materials Park, Ohio, USA, Release 2015/16.

[14] R.F. Domagala, D.J. McPherson, M. Hansen, System zirconium-nitrogen, Trans. AIME 8 (1956) 98–105.

[15] H. Nowotny, E. Rudy, F. Benesovsky, Untersuchungen in den systemen: hafnium-bor-kohlenstof und zirkonium-bor-kohlenstofv, Mon. Chem. 92 (1961) 393–402.

[16] E.I. Smagina, V.S. Kutsev, B.F. Ormont, Equilibrium studies of the system Zr-N at high temperatures, Zhur. Fiz. Khim. 34 (1960) 2328–2335.

[17] G.M. Kibler, T.F. Lyon, V.J. Desantis, Rep. Air Force Contract AF-33, (616)-6841 (March 1962)

[18] G.V. Samsonov, T.S. Verkhoglyadova, Physical properties of zirconium nitride in the homogenity region, Dop. Akad. Nauk. RSR 1 (1962) 48–50.

[19] E.I. Gal'braikh, O.P. Kulik, A.A. Kuznetsov, M.D. Lyutaya, M.P. Morozova, Enthalpy of formation of the nitrogen solid solution in α-zirconium and of zirconium nitride in their homogeneity regions, Powder Metall. Met. Ceram. 9 (1970) 748–751.

[20] M. Hoch, D.P. Dingledy, H.L. Johnston, The vaporization of TiN and ZrN, J. Am. Chem. Soc. 77 (1955) 304–306.

[21] A.D. Mah, N.L. Gellert, Heats of formation of niobium nitride, tantalum nitride and zirconium nitride from combustion calorimetry, J. Am. Chem. Soc. 78 (14) (1956) 3261–3263.

[22] H.A. Solman, C.A. Harvey, O. Kubasehewski, Fundamental reactions in the vacuum-fusion method and its application to the determination of O_2, N_2 and H_2 in Mo, Th, Ti, U, V and Zr, J. Inst. Met. 80 (1951) 1360.

[23] D.D. Wagman, W.H. Evans, V.B. Parker, I. Halow, Selected values of chemical thermodynamic properties, Natl. Bur. Stand., U. S., Tech. Note (1971) 270–275.

[24] A.S. Bolgar, V.F. Litvinenko, L.A. Kizhikina, I.I. Timofeeva, O.P. Kulik, High-temperature thermodynamic characteristics of zirconium mononitride in its homogeneity range, Porosh. Metall. 11 (1976) 48–53.

[25] S.S. Todd, Heat capacities at low temperatures and entropies of zirconium, zirconium nitride, and zirconium tetrachloride, J. Am. Chem. Soc. 72 (1950) 2914–2915.

[26] J.P. Coughlin, E.G. King, High-temperature heat contents of some zirconium-containing substances, J. Am. Chem. Soc. 72 (5) (1950) 2262–2265.

[27] P. Duwez, F. Odell, Phase relationships in the binary systems of nitrides and carbides of zirconium, columbium, titanium, and vanadium, J. Electrochem. Soc. 97 (1950) 299–304.

[28] G.Y. Yang, E. Etchessahar, J.P. Bars, R. Portier, J. Debuigne, A miscibility gap in the fcc δ-nitride region of the ternary system titanium-zirconium-nitrogen, Scr. Metall. Mater. 31 (1994) 903–908.

[29] E. Etchessahar, J. Bars, D. Ansel, The partial ($Ti_{0.5}$ $Zr_{0.5}$)-N phase diagram from 0 to 50 at.%, J. Alloys Compd. 335 (2002) 126–131.

[30] A. Hörling, J. Sjölén, H. Willmann, T. Larsson, M. Odén, L. Hultman, Thermal stability, microstructure and mechanical properties of $Ti_{1-x}Zr_xN$ thin films, Thin Solid Films 516 (2008) 6421–6431.

[31] A. Wang, S.-L. Shang, Y. Du, L. Chen, J. Wang, Z.-K. Liu, Effects of pressure and vibration on the thermal decomposition of cubic Ti1-x Al x N, Ti1-x Zr x N, and Zr1-x Al x N coatings: a first-principles study, J. Mater. Sci. 47 (2012) 7621–7627.

[32] P. Ou, J. Wang, S. Shang, L. Chen, Y. Du, Z.-K. Liu, F. Zheng, A first-principles study of structure, elasticity and thermal decomposition of Ti 1- x TMxN alloys (TM= Y, Zr, Nb, Hf, and Ta), Surf. Coat. Technol. 264 (2015) 41–48.

[33] A.T. Dinsdale, SGTE data for pure elements, Calphad 15 (1991) 317–425.

[34] Y.M. Muggianu, M. Bambino, J.P. Bros, Enthalpy of formation of liquid Bi-Sn-Ga alloys at 723 K, choice of an analytical expression of integral and partial excess quantities of mixing, J. Chim. Phys. 72 (1973) 83–88.

[35] O. Redlich, A.T. Kister, Algebraic representation of thermodynamic properties and the classification of solutions, Ind. Eng. Chem. 40 (1948) 345–348.

[36] G. Kresse, J. Furthmüller, Efficient iterative schemes for ab initio total-energy calculations using a plane-wave basis set, Phys. Rev. B 54 (1996) 11169.

[37] G. Kresse, J. Furthmüller, Efficiency of ab-initio total energy calculations for metals and semiconductors using a plane-wave basis set, Comput. Mater. Sci. 6 (1996) 15–50.

[38] MedeA Version 2.10, Materials Design 2012, Angel Fire, New Mexico. URL ⟨http://www.materialsdesign.com/⟩

[39] A. Zoroddu, F. Bernardini, P. Ruggerone, V. Fiorentini, First-principles prediction of structure, energetics, formation enthalpy, elastic constants, polarization, and piezoelectric constants of AlN, GaN, and InN: comparison of local and gradient-corrected density-functional theory, Phys. Rev. B 64 (2001) 045208.

[40] P.E. Blöchl, Projector augmented-wave method, Phys. Rev. B 50 (24) (1994) 17953.

[41] G. Kresse, D. Joubert, From ultra soft pseudopotentials to the projector augmented-wave method, Phys. Rev. B 59 (1999) 1758.

[42] J.P. Perdew, K. Burke, M. Ernzerhof, Generalized gradient approximation made simple, Phys. Rev. Lett. 77 (1996) 3865.

[43] H.J. Monkhorst, J.D. Pack, Special points for brillouin-zone integrations, Phys. Rev. B 13 (1976) 5188.

[44] P.E. Blöchl, O. Jepsen, O.K. Andersen, Improved tetrahedron method for Brillouin-zone integrations, Phys. Rev. B 49 (1994) 16223.

[45] A. Zunger, S.-H. Wei, L.G. Ferreira, J.E. Bernard, Special quasirandom structures, Phys. Rev. Lett. 65 (1990) 353.

[46] A. Van de Walle, P. Tiwary, M. De Jong, D. Olmsted, M. Asta, A. Dick, D. Shin, Y. Wang, L.-Q. Chen, Z.-K. Liu, Efficient stochastic generation of special quasirandom structures, Calphad 42 (2013) 13–18.

[47] A. Van de Walle, M. Asta, G. Ceder, The alloy theoretic automated toolkit: A user guide, Calphad 26 (2002) 539–553.

[48] K. Parlinski, Z. Li, Y. Kawazoe, First-principles determination of the soft mode in cubic ZrO_2, Phys. Rev. Lett. 78 (1997) 4063.

[49] A. Togo, I. Tanaka, First principles phonon calculations in materials science, Scr. Mater. 108 (2015) 1–5.

[50] C. Qiu, S.M. Opalka, G.B. Olson, D.L. Anton, The Na-H system: from first-principles calculations to thermodynamic modeling, Int. J. Mat. Res. 97 (2006) 845–853.

[51] K.K. Irikura, Experimental vibrational zero-point energies: diatomic molecules, J. Phys. Chem. Ref. Data 36 (2) (2007) 389–397.

[52] B. Jansson, (Ph.D. thesis), Division of Physical Metallurgy, Royal Institute of Technology, Stockholm, Sweden,.

[53] B. Sundman, B. Jansson, J.O. Andersson, The thermo-calc databank system, Calphad 9 (1985) 153–190.

[54] K.C. Hari Kumar, P. Wollants, Some guidelines for thermodynamic optimisation of phase diagrams, J. Alloy. Compd. 320 (2001) 189–198.

[55] H. Okamoto, The Hf-N (hafnium-nitrogen) system, Bull. Alloy Phase Diagr. 11 (1990) 146–149.

[56] P. Farrar, S. Adler, On the system titanium-zirconium, Trans. Met. Soc. AIME 236 (1966) 1061–1064.

[57] E. Rudy, Compilation of phase diagram data, Technical Rept. AFML-TR-65-2, Part V, Wright Patterson Air Force Base, 1969.

[58] D. Chatterji, M. Hepworth, S. Hruska, On the system Ti-Zr, Metall. Trans. 2 (1971) 1271–1272.

[59] J. Etchessahar, J. Debuigne, Study of the allotropic transformation in equiatomic titanium-zirconium alloys: influence of purity of the materials and nitrogen on the phase transition, Mem. Sci. Rev. Metall. 74 (3) (1977) 195–205.

[60] J.-P. Auffredic, E. Etchessahar, J. Debuigne, Remarques sur le diagramme de phases Ti-Zr: Étude microcalorimétrique de la transition, J. Less-Common Met. 84 (1982) 49–64.

[61] J. Blacktop, J. Crangle, B. Argent, The $\alpha \rightarrow \beta$ transformation in the Ti-Zr system and the influence of additions of up to 50 at.% Hf, J. Less-Common Met. 109 (1985) 375–380.

[62] M. Ruch, D. Arias, Comments on the equilibrium diagram of the Ti-Zr system, Scr. Metal. Mat. 29 (1993) 533–538.